Experiments on and thermodynamic analysis of a turbocharged engine with producer gas as fuel

S Dasappa[1]*, **H V Sridhar**[2], and **I Muzumdar**[3]
[1]Centre for Sustainable Technologies, Indian Institute of Science, Bangalore, India
[2]Combustion Gasification and Propulsion Laboratory, Department of Aerospace Engineering, Indian Institute of Science, Bangalore, India
[3]GE Energy, India

The manuscript was received on 31 March 2011 and was accepted after revision for publication on 14 July 2011.

DOI: 10.1177/0954406211419063

Abstract: This article presents the studies conducted on turbocharged producer gas engines designed originally for natural gas (NG) as the fuel. Producer gas, whose properties like stoichiometric ratio, calorific value, laminar flame speed, adiabatic flame temperature, and related parameters that differ from those of NG, is used as the fuel. Two engines having similar turbochargers are evaluated for performance.

Detailed measurements on the mass flowrates of fuel and air, pressures and temperatures at various locations on the turbocharger were carried out. On both the engines, the pressure ratio across the compressor was measured to be 1.40 ± 0.05 and the density ratio to be 1.35 ± 0.05 across the turbocharger with after-cooler. Thermodynamic analysis of the data on both the engines suggests a compressor efficiency of 70 per cent. The specific energy consumption at the peak load is found to be 13.1 MJ/kWh with producer gas as the fuel. Compared with the naturally aspirated mode, the mass flow and the peak load in the turbocharged after-cooled condition increased by 35 per cent and 30 per cent, respectively. The pressure ratios obtained with the use of NG and producer gas are compared with corrected mass flow on the compressor map.

Keywords: producer gas, turbocharger, gas engines, gasification

1 INTRODUCTION

The use of renewable energy source for power generation is gaining momentum and, in particular, important for distributed power generation. This aspect is further becoming important owing to the climate change mitigation requirements in several advanced countries and possible mitigation options for countries with a high demand–supply gap. India, which is also playing a key role in the mitigation options, has several programmes for power generation using various sources of renewable energy [**1**].

Biomass gasification, a thermo-chemical conversion process, is an important technology package that has drawn attention from various stakeholders to meet the requirements of captive, grid, or any distributed grid networks. Producer gas is generated from biomass through a thermo-chemical conversion process known as gasification in which solid biomass is converted to gaseous fuel [**2**–**5**]. Gasification consists of drying, pyrolysis, oxidation, and reduction, and it is a fuel-rich combustion process occurring under substoichiometric conditions. The gasification process results in a fuel gas with 18–20 per cent each of H_2 and CO and 2 per cent CH_4, with the rest being inert gases like CO_2 and N_2. The lower calorific value of the gas is in the range 4.7 ± 0.2 MJ/kg, with the stoichiometric air–fuel ratio being 1.3 ± 0.05 on mass basis.

*Corresponding author: Centre for Sustainable Technologies, Indian Institute of Science, Bangalore 560012, India.
email: dasappa@cgpl.iisc.ernet.in

The use of producer gas in an internal combustion engine has been possible in dual-fuel and gas-alone modes [**3**–**9**]. With advanced research in the area of internal combustion engines towards improving the power output-to-weight ratio, several developments have taken place [**10**]. Of the several pathways considered towards improving the power and efficiency, turbochargers have played a critical role. Further, the extent of power enhancement depends on the pressure ratio of the compressor and also on the in-cylinder process limitation arising from the rate of pressure rise.

The use of producer gas as a fuel has been limited to a few research groups and very little research in adapting fossil fuel-designed engines for producer gas applications has been reported. Some of these aspects have been analysed by earlier researchers [**3**, **9**, **11**–**19**]. Tinaut *et al.* [**12**] have carried out analysis to predict the engine performance using Engine Fuel Quality (EFQ) which is the combined effect of stoichiometric air–fuel ratio and stoichiometric mixture heating value, both depending on the producer gas composition. The estimation of engine power made using the EFQ parameter indicates that power at full load is reduced at about two-thirds of the maximum obtained with a conventional liquid fuel. They use some of the results of the work done by the present authors for the analysis. Ahrenfeldt *et al.* [**13**] have presented results for a small capacity engine with and without supercharging and have shown an increase in power output and efficiency with supercharging.

Table 1 compares the properties of producer gas with other fuels, like natural gas (NG) and liquefied petroleum gas (LPG). Critical properties that influence performance of the engine relating to the combustion processes inside the cylinder are the laminar flame speed, adiabatic flame temperature, stoichiometric ratio, flammability limits, etc. From Table 1, it is evident that the properties of producer gas are significantly different from those of fossil fuels. The laminar flame speed at stoichiometry for producer gas is 30 per cent higher than for NG and 10 per cent higher than for LPG. This is mainly due to the presence of hydrogen whose laminar flame speed at stoichiometric condition with air is 2.6 m/s. Similarly, the adiabatic flame temperature is lower for producer gas compared with those of other gaseous fuels. The other important parameter is the product-to-reactant mole ratio, which is less than unity for producer gas, resulting in lower cylinder pressures. It is argued that these factors contribute to the de-rating of a NG engine when operated with producer gas [**14**]. Sridhar [**15**] has addressed the importance of these properties in optimizing engine performance. Sridhar *et al.* [**15**] also present results where the cylinder peak pressures using producer gas are lower compared with those for fossil fuel operation.

Studies suggest that the power de-rating is in the range 30–35 per cent with producer gas as the fuel compared with the fossil fuel-rated capacity. The overall combustion processes within the engine cylinder have an influence on the turbocharger performance, which in turn would affect the power output. This study focuses on the preliminary performance evaluation of turbochargers using producer gas as the fuel using engines manufactured by Cummins India Limited, designed for operating on NG as the fuel. These studies are carried out to establish the performance of the turbocharger with respect to the compressor pressure ratio at various load conditions and also derive other parameters from the detailed experiments and analysis. Thermodynamic analysis is carried out to establish the compressor and turbine efficiencies. Both pressure and density ratios are compared with those for NG operation.

2 MATERIALS AND METHODS

The engines used for tests are manufactured by Cummins India Limited, designed for NG operation. These engines have been used with producer gas as fuel for power generation and operated for over 10 000 h [**4**, **5**]. The specifications of the two spark-ignited gas engines are presented in Table 2 [**20**, **21**]. Engines 1 and 2 have the same turbocharger(s), ignition systems, governing system, bore, and stroke. The turbocharger is 4 LGK-557 from HOLSET. Engine

Table 1 Comparison of properties of standard fuels with producer gas

Properties	Producer gas	NG	LPG
Chemical composition	Mixture of CO, CO_2 CH_4, H_2, N_2	CH_4	C_3H_8, C_4H_{10}
Fuel, LCV (MJ/kg)	5.0	50.2	47
Fuel, LCV (MJ/Nm^3)	5.6	35.8	93
Air–fuel ratio at $\varphi = 1$ (mass)	1.35	17.2	15.5
Energy density of $A + F$ mixture (MJ/kg)	2.12	2.76	2.78
Laminar flame speed at stoichiometry (m/s)	0.50	0.35	0.44
Peak flame temperature (K)	1800	2210	2250
Product–reactant mole ratio	0.89	1.0	1.0

Table 2 Specification of the engines

Parameter	Engine 1	Engine 2
Make and model	Cummins, GTA-1710-G	Cummins, GTA-855-G
Engine type	'V' configuration 12 cylinder, turbocharged with after-cooler gas engine	In-line, six cylinder, turbocharged with after-cooler gas engine
Bore (mm)	140	140
Stroke (mm)	152	152
Total displacement (L)	28	14
CR	10	8.5
Engine rating with NG as fuel at 1500 r/min (kW)	355	168
Conversion/modification, if any	Producer gas carburettor adapted	Producer gas carburettor adapted

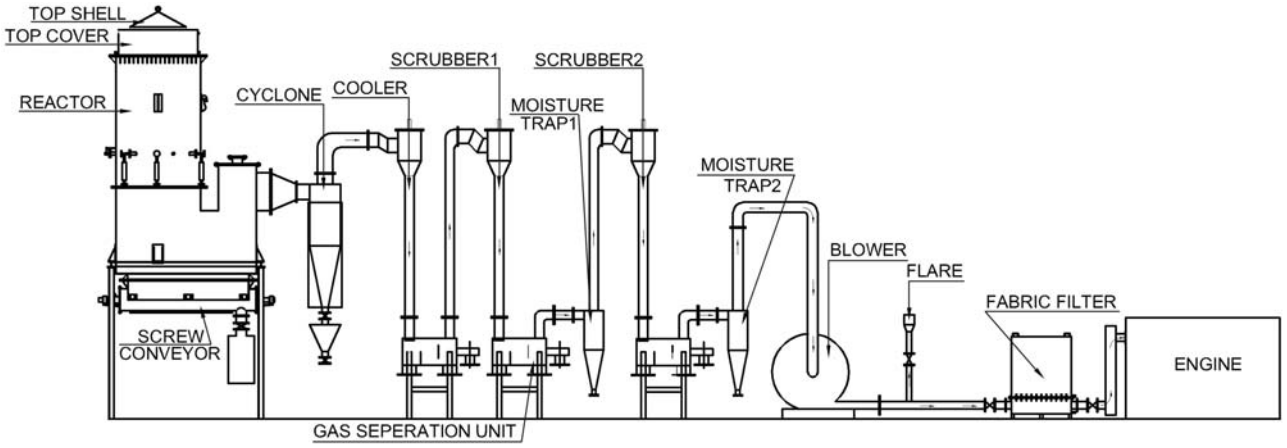

Fig. 1 Schematic of the gasification system

1 is a 12-cylinder 'V' configuration, while Engine 2 is an inline system. The compression ratio (CR) of Engine 1 is 10, whereas that of Engine 2 is 8.5, which will slightly affect the power output.

These engines were operational at two different locations with Engine 1 being a grid-linked application and Engine 2 used for captive power generation [**22**]. Both the engines were fitted with a special producer gas carburettor [**15**, **22**] for ensuring constant A/F over the complete load range.

The engines were coupled to biomass gasification systems of appropriate capacity to generate engine quality gas [**4**, **5**]. Details of the gasification system are elaborated in reference [**2**]. In brief, the gasification system is an open-top downdraft gasifier, with a cooling and cleaning system to generate clean gas. Producer gas quality plays an important role in the operability of the engines fitted with turbochargers. The presence of tar and particulates in significant quantity (greater than 25 mg/m^3) influences the performances of the compressor and after-cooler by blockages created due to deposition. These aspects have been addressed in the gasification system to maintain low tar and particulate levels (less than 10 mg/m^3) in the gas.

In brief, Engine 1 was part of a 1-MW power station using producer gas which had five producer gas engines, connected in parallel to a common bus and through it to the grid [**4**]. Two gasifiers using coconut shells as biomass fuelled these five gas engines. Engine 2 was coupled to a gasifier of 150 kg/h for captive power generation in a textile industry [**22**]. The industry had a facility to gradually load the engine. This gasifier was fuelled using coconut shells during the tests.

Figure 1 shows the typical schematic of the gasification system used during the tests. The novel open-top downdraft reactor design is a ceramic-lined cylindrical vessel with a bottom screw for ash extraction. The screw-based ash extraction system allows for extracting the residue at a predetermined rate. In brief, the reactor has air nozzles and open top for air to be drawn into the system. The gas conditioning system involves cyclone, scrubbers, and fabric filter. The gas is de-humidified or dried using the principle

of condensate nucleation to reduce the moisture and fine contaminants. A blower provides the necessary suction for meeting the engine requirements. The dual air entry – from top and the nozzles – permits establishment of front moving propagation towards the top of the reactor to establish a large thermal bed inside the reactor and improve the residence time [**2**]. The details of the gasification technology are discussed in reference [**5**].

2.1 Measurement scheme

To study the performance characteristics of the turbocharger, some thermodynamic properties were measured and others deduced. Several sets of measurements were conducted on both the engines. Measurements were made on continuous operation engines and the major parameters recorded during the performance evaluation are:

(a) gas and mixture composition;
(b) gas and air flowrate;
(c) exhaust composition;
(d) temperature across the turbocharger and aftercooler;
(e) pressure across the turbocharger and aftercooler;
(f) electrical load on the engine generator system.

Online gas analysers from SICK-Maihak, using non-dispersive infrared and thermal conductivity detector-based instruments, were used in gas and mixture composition measurement. The gas and air flow measurement was carried out through hot wire anemometer and Pitot tubes. Quintox make exhaust analyser was used for measuring exhaust composition. K-type thermocouples were used in temperature measurements and pressure transducers based on piezoresistive sensitive elements (KIMO instruments) with an accuracy of ± 1.5 per cent were used for pressure measurements.

The measurement scheme used in this study is as shown in Fig. 2. Measurements were made on the engine only after the gasifier operations were stabilized, i.e. steady-state conditions were attained with respect to consistent quality gas. All the experiments were repeated at different loads. The producer gas composition was monitored during the period of experimentation.

3 THE EXPERIMENTS

Experiments were conducted at two field locations where the ambient temperature was in the range 310 ± 5 K. Engine 1 was located at a place 410 m above mean sea level, while Engine 2 was located at a place 310 m above mean sea level.

Figure 3 depicts the gas compositions of producer gas at both the sites with respect to load. The composition is nearly the same at both the locations with percentages of CO: 20 ± 1, H_2: 19 ± 1, CH_4: 1.5 ± 0.2, CO_2: 12 ± 1, and the rest N_2. The average calorific value is 4.6 ± 0.1 MJ/kg. This ensures nearly constant quality of the fuel used in both the engines. The

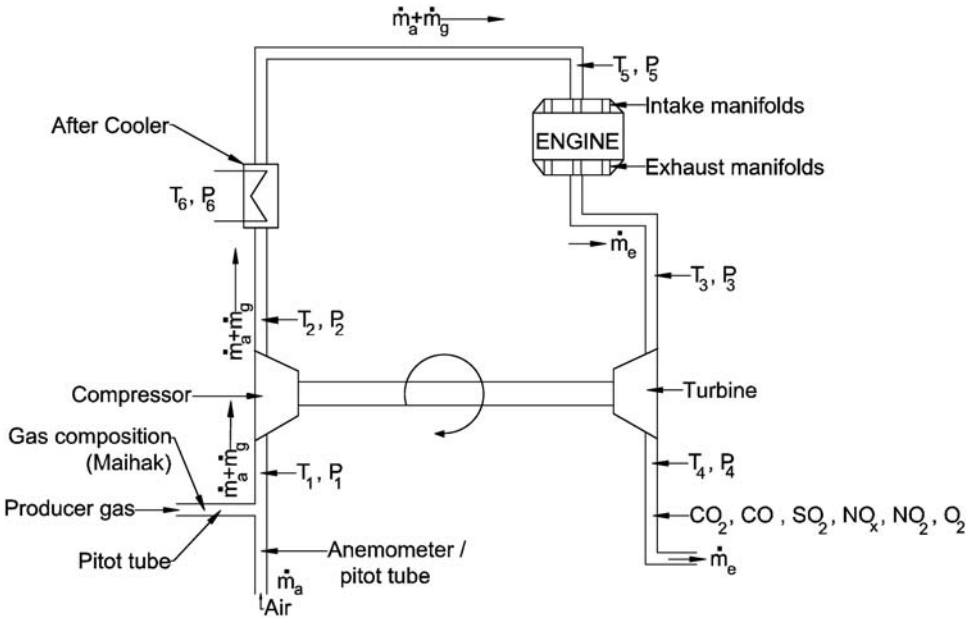

Fig. 2 Schematic of the measurement plan

stoichiometric air requirement for the above gas composition is in the range of 1:1.25.

Holset 4 LGK/557 turbocharger was used in both the engines. The only difference is that Engine 1 had two separate turbochargers fitted to different cylinder banks in the 'V' configuration, 12 cylinders, turbocharged with after-cooler and Engine 2 had a single turbocharger fitted to an in-line, 6 cylinders, turbocharged with after-cooler.

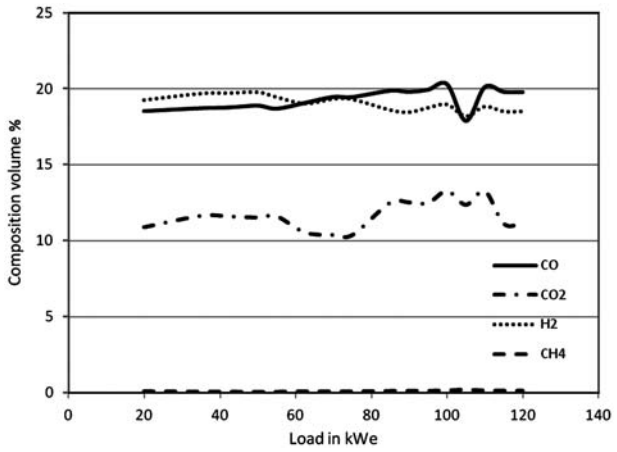

Fig. 3 Gas composition at various loads, Engine 1

Tables 3 and 4 summarize the results from measurements conducted on Engines 1 and 2. These are averages of several sets of experiments. The mass flowrates of gas and air are represented as $\dot{m}_g$ and $\dot{m}_a$, respectively; $\dot{m}_a$ is the total mass flow exiting from the engine exhaust. T_1 to T_5 and P_1 to P_5 are the temperature and pressure measurements on the turbocharger.

All the measurements were made on a single turbocharger for Engine 1. For brevity, it is assumed that the actual flow through each of the turbochargers is one-half of the total flow the engine is drawing. This effectively means that each of the turbochargers would handle one-half the flowrate of total gas air mixture. On this basis, it is assumed that each turbocharger coupled to a set of six cylinders supports half the total load that the engine is capable of. From the specification of Engine 1 as in Table 2, it is clear that the flow through the turbocharger can generate about 120 kW. Table 3 provides the details on load, mass flowrate of air and gas, along with the calculated pressure ratios for Engine 1 for one turbocharger. The

Table 3 Compressor flow and pressure measurements at various loads on Engine 1

Load per turbo (kW)	Gas flow, $\dot{m}_g$ (kg/s)	Air flow, $\dot{m}_a$ (kg/s)	Compressor flow (kg/s)	A/F	P_2/P_1	Specific energy consumption (MJ/kWh)
20.00	0.018	0.026	0.043	1.44	0.766	14.6
30.00	0.031	0.044	0.075	1.428	0.819	16.7
37.50	0.036	0.052	0.087	1.440	0.928	15.6
40.00	0.042	0.060	0.103	1.434	1.133	17.0
45.00	0.046	0.068	0.114	1.468	1.153	16.6
50.00	0.053	0.076	0.128	1.43	1.191	17.2
62.50	0.059	0.084	0.143	1.417	1.210	15.3
75.00	0.063	0.089	0.152	1.406	1.227	13.6
82.50	0.068	0.100	0.169	1.468	1.239	13.4
87.50	0.072	0.101	0.173	1.394	1.257	13.3
92.50	0.076	0.104	0.180	1.354	1.311	13.3
100.0	0.081	0.109	0.190	1.354	1.332	13.1
105.0	0.085	0.115	0.199	1.360	1.337	13.1
110.0	0.089	0.116	0.205	1.314	1.363	13.1
115.0	0.093	0.121	0.214	1.309	1.385	13.1

Table 4 Compressor flow and pressure measurements at various loads on Engine 2

Load (kW)	Gas flow $\dot{m}_g$ (kg/s)	Air flow $\dot{m}_a$ (kg/s)	Compressor flow (kg/s)	A/F	P_2/P_1	Specific energy consumption (MJ/kWh)
0	0.023	0.038	0.061	1.65	1.011	
20	0.018	0.029	0.046	1.61	1.065	14.6
30	0.026	0.040	0.066	1.50	1.131	14.0
45	0.038	0.056	0.094	1.47	1.257	13.7
50	0.042	0.063	0.105	1.49	1.266	13.6
60	0.051	0.077	0.128	1.52	1.302	13.8
70	0.059	0.074	0.133	1.25	1.304	13.6
80	0.067	0.082	0.149	1.21	1.376	13.6
90	0.072	0.087	0.159	1.20	1.429	13.0
100	0.081	0.100	0.181	1.24	1.438	13.1
110	0.089	0.106	0.195	1.20	1.455	13.1

mass flow at 115 kW per turbocharger is about 0.214 kg/s with a pressure ratio of 1.39 for Engine 1.

Similarly, Table 4 provides the mass flowrates of air and gas into the engine from the turbo compressor along with the calculated pressure ratios for Engine 2. At 110 kW, the total flow is 0.195 kg/s and compressor pressure ratio 1.46. In both the cases, the A/F is found to be in the range 1.35 ± 0.2. The specific energy consumption (SEC), a manifestation of the engine efficiency, defined as the energy input from the gaseous fuel to generate 1 kWh of electricity, was found to 13.1 MJ/kWh at the peak load. This value of SEC translates to an engine efficiency of 28 per cent from gas to electricity.

Table 5 provides the details of the mixture composition before entering the engine manifold for Engine 1. On carrying out the elemental balance, the A/F based on varying load suggests that the exhaust oxygen varies from about 5 per cent at low load to about 1.5–2 per cent at the higher loads. This is consistent with the design of the carburettor. The A/F is found to be in the range 1.35 ± 0.1, which is consistent with the A/F measured from the gas and air flowrates.

4 THE ANALYSIS

Figure 4 shows the typical temperature/entropy diagram for a turbocharger. The measurement scheme adapted in this study is aimed at obtaining relevant thermodynamic properties and it establishes the performance of the compressor and the turbine.

Work done by the compressor and the turbine can be calculated by

$$W_c = C_{\mathrm{p}}(T_2 - T_1)\mathrm{kJ/kg}$$

and

$$W_t = C_{\mathrm{p}}(T_3 - T_4)\mathrm{kJ/kg}$$

where W_c is the compressor work, W_t the turbine work, and T_1, T_2, T_3, T_4, and T_5 the temperatures at different locations in the turbocharger and aftercooler.

The total flow is the sum of air and gas flows through the engine, which is the same as mass flow through the compressor and turbine. The compressor work $= \dot{m}\, C_{\mathrm{p}12}(T_2 - T_1)$ and the turbine work $= \dot{m}\, C_{\mathrm{p}34}(T_3 - T_4)$, where $\dot{m}_c =$ mass flowrate through the turbocharger, which is the sum of $\dot{m}_g$ and $\dot{m}_a$.

The isentropic efficiency of the compressor is the ratio of the power that would be necessary to operate the compressor in an ideal adiabatic situation to the actual power that is necessary to operate the compressor. Therefore, η_c, the compressor isentropic efficiency is

$$\eta_c = \frac{h_{2s} - h_1}{h_2 - h_1} = \frac{T_{2s} - T_1}{T_2 - T_1} \tag{1}$$

In the above expressions, C_{p} is the specific heat at constant pressure and considered constant, T_{2s} the isentropic temperature, T_2 and T_1 the stagnation temperatures before and after the compressor.

In a similar manner, the isentropic efficiency of the turbine η_t of the turbocharger is defined as the ratio between the power produced by a real turbine to the power produced by an ideal turbine and is given by

$$\eta_t = \frac{h_3 - h_4}{h_3 - h_{4s}} = \frac{T_3 - T_4}{T_3 - T_{4s}} \tag{2}$$

where C_{p} is considered constant, T_{4s} isentropic temperature, and T_3 and T_4 the stagnation temperatures before and after the turbine.

Table 5 Gas composition of the mixture entering the engine manifold for Engine 1

	Mixture gas composition (vol%)					
Load	CO	CO_2	CH_4	O_2	H_2	N_2 by difference
20	8.5	4.3	0.2	13.9	7.8	0.52
35	8.7	4.5	0.2	12.7	8.1	0.47
43	8.7	4.7	0.2	12.9	8.0	0.48
50	8.7	4.5	0.2	12.8	7.9	0.48
55	8.6	4.4	0.2	13.0	7.8	0.48
63	9.0	4.1	0.1	13.7	7.7	0.51
70	9.0	4.0	0.1	13.8	7.6	0.51
75	9.2	4.1	0.1	13.5	8.0	0.50
85	9.4	5.2	0.4	13.5	7.9	0.51
90	9.5	5.3	0.4	13.6	8.0	0.51
95	9.2	5.1	0.4	13.6	7.8	0.51
100	9.1	5.2	0.4	13.7	7.7	0.51
105	7.7	4.5	0.5	14.5	6.6	0.55
110	7.9	4.0	0.2	15.1	6.3	0.57
115	7.9	4.0	0.3	15.2	6.3	0.57
120	7.9	4.0	0.3	15.1	6.3	0.57

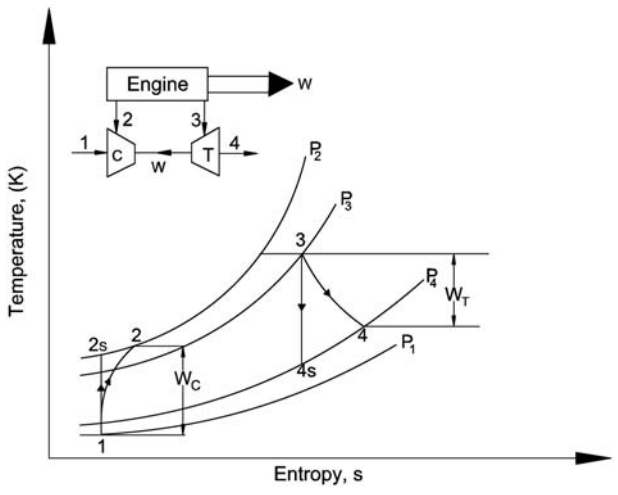

Fig. 4 Typical temperature–entropy diagram for a turbocharger

In a turbocharger, the compressor is driven solely by the turbine, and mechanical efficiency η_m can be defined as

$$\eta_m = \frac{\text{Compressor work}}{\text{Turbine work}} = \frac{W_c}{W_t}$$

4.1 Mass flow and pressure ratio

Engine 2 has a nameplate capacity of 168 kW with turbocharger after-cooled configuration using NG as the fuel. The same engine under natural aspiration is rated for 130 kW [**21**]. On the basis of the cylinder displacement capacity of 14 L and the engine speed at 1500 r/min, the total mass flow of gas and air under natural aspirated condition is estimated at 0.140 kg/s at 90 per cent volumetric efficiency. The measured mass flowrates in the turbocharged after-cooled configuration as indicated in Tables 1 and 2 are in the range 0.195–0.215 kg/s for both the engines evaluated. It is clear that the total mass flow has increased by about 36 per cent in turbocharged mode compared with naturally aspirated mode. The difference in mass flowrates of gas and air mixture drawn into the two engines is about 5 per cent and within the range of experimental errors.

Figure 5 shows the variation of compressor pressure ratio with load for both the engines. It is important to mention that Engine 1, which is rated for 240-kW electrical load with producer gas as fuel, has two turbochargers, in effect each turbocharger contributing about 120 kW. In view of this, it is easy to compare it with Engine 2, which is a 120-kW capacity engine with one turbocharger. As the load increases, the pressure ratio increases and reaches a maximum at full load. The pressure ratios achieved at similar load conditions for the two engines are nearly the same. At lower loads between 20 and 42 kW, the pressure ratio is lower than unity. A maximum pressure ratio of 1.39 was obtained at the highest load of 115 kW for Engine 1 and 1.46 at 110 kW for Engine 2.

4.2 Effectiveness of the after-cooler

The after-cooler is made of aluminium-finned copper tube exchanger with gas passages of the order of about 0.5 mm. From the experimental results, it was observed that at all loads, the after-cooler outlet temperature was in the range 294–419 K depending upon the load on both the engines. Figure 6 shows the performance of the after-cooler. The temperature drop realized across the after-cooler in both engines is about 35 K at nearly the rated load, implying that the performances of the two after-coolers fitted on different engines is nearly the same.

The pressure ratio for the compressor and after-cooler for Engine 2 is depicted in Fig. 7. The small reduction in pressure ratio (P_5/P_1) is due to the resistance across the after-cooler. At 115 kW, the pressure drop across the after-cooler is about 550 Pa,

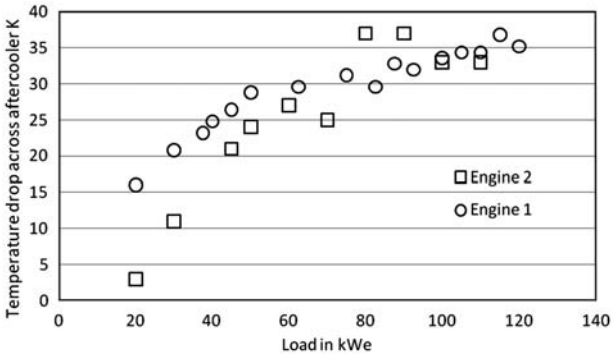

Fig. 6 After-cooler performance for Engines 1 and 2

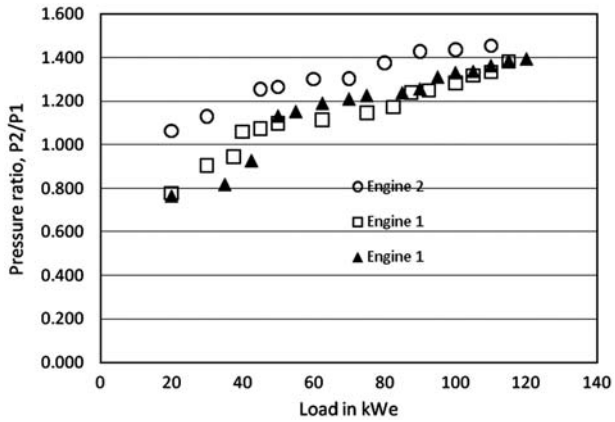

Fig. 5 Comparison of pressure ratios with load for both the engines

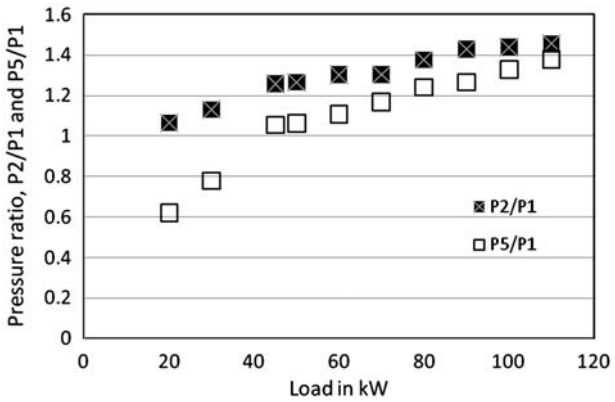

Fig. 7 Effect of after-cooler on pressure ratio (Engine 2)

consistent with the manufacturer's data. The gas air mixture enters the engine manifold at nearly 142 kPa.

4.3 Density ratio

The purpose of turbocharging is to increase the engine output by increasing the density of the mixture (air and gas) drawn into the engine. It was found that the density ratio of the mixture increases with load and was 1.28 at the maximum load achieved for Engine 2. Figure 8 illustrates the effect of the after-cooler on the density ratio. As a consequence of gas air mixture cooling, the density ratio improves with load. The temperature of the mixture at the exit of the after-cooler is lower by about 35 K at the 115 kW load. Figure 8 presents the plot of the density ratio across the compressor and the after-cooler with respect to the ambient pressure. It is clear that beyond 65 kW, the cooling effect increases the density of the gas air mixture and at the rated condition, the density ratio is higher than what is achieved across the compressor. With increase in mass flowrate, the heat transfer processes improve between gas and water, thus improving the density of the gas air mixture and hence the density ratio. At 110 kW, the presence of the after-cooler increases the density ratio to 1.35 as against 1.27 before the after-cooler.

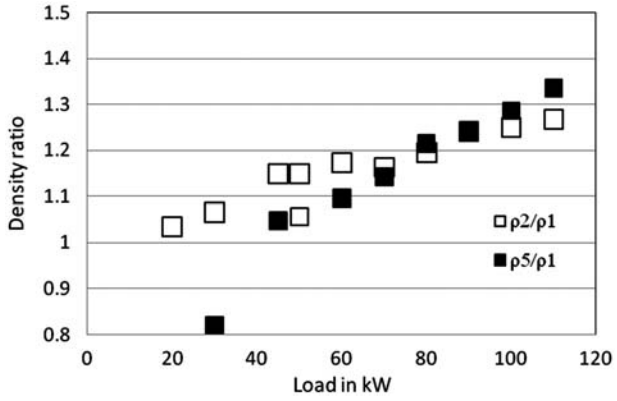

Fig. 8 Effect of density ratio before and after the after-cooler (Engine 2)

Table 6 Compressor performance parameters of Engine 2

Load (kW)	P_5/P_1	T_{2s} (K)	η_c	Compressor power (kW)
0	0.431	309.0	0.34	0.29
20	0.621	313.6	0.62	0.98
30	0.779	320.1	0.58	2.42
45	1.054	329.9	0.72	4.29
50	1.063	326.3	0.69	4.58
60	1.106	334.3	0.72	5.42
70	1.168	330.1	0.69	6.06
80	1.240	339.6	0.70	8.18
90	1.265	343.3	0.71	8.47
100	1.328	338.4	0.73	8.72
110	1.380	339.5	0.77	8.94

5 RESULTS AND DISCUSSIONS

The turbochargers are selected by first defining the compressor stage (to meet the engine requirements) and then designing a turbine stage to 'match' the compressor and engine. Turbocharger efficiency is the combined effect of both compressor and turbine efficiency. Considering this, measurements were carried out on the turbine side also. All the measurements were made simultaneously along with the compressor side for various loads.

On the basis of the experimental investigations, the performances of the compressor and turbine were evaluated. The derived data from all the experimental data are analysed to evaluate the thermodynamic parameters necessary to estimate the performance of the compressor and turbine.

5.1 Compressor efficiency

Table 6 provides the values of pressure ratio (P_5/P_1) between the compressor and the after-cooler along with the isentropic temperature at various load conditions for Engine 2. At 110 kW, the pressure ratio is 1.38.

The compressor efficiency is estimated using $\eta_c = \frac{T_{2s}-T_2}{T_2-T_1}$. It is observed that the efficiency gradually increases with load, reaching about 77 per cent at 110 kW for Engine 2. Estimated compressor work is about 8.9 kW at 110 kW, which amounts to less than 10 per cent of the engine output.

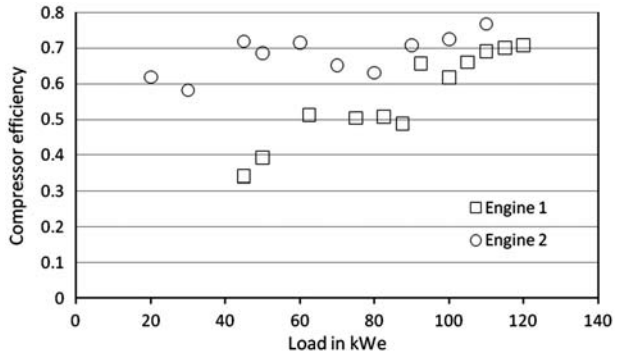

Fig. 9 Comparison of compressor efficiencies of Engines 1 and 2

Figure 9 shows the plot of compressor efficiency with respect to the load for both the engines. The compressor efficiency of the larger engine, i.e. Engine 1, is lower at lower load and is about 71 per

cent at 115 kW, while in the case of Engine 2, the peak efficiency is about 77 per cent. However, comparing the data obtained on Engines 1 and 2, Engine 2 operated at a slightly higher pressure ratio than Engine 1 under all loads, and the mass flowrate of Engine 1 is slightly greater than that of Engine 2.

5.2 Turbine efficiency

For estimating turbine isentropic efficiency; turbine expansion and isentropic temperature ratios were used. The turbine efficiency is calculated using equation (2).

The use of measured temperature data yielded turbine efficiency of more than 100 per cent at almost all loads. In order to understand this discrepancy, the entire turbocharger construction was reviewed. Close examination revealed that in both the gas engines, jacket cooling is enabled on the turbine side to control the overall temperature and thereby improving the life. It is clear that water flow removes some of the heat and hence the measured temperature is less than isentropic temperature ($T_{4s} = T_3(P_4/P_3)^{(\gamma-1)/\gamma}$).

A simple analysis was carried out to account for the turbine performance. The only thermodynamic parameters that have an effect are turbine outlet pressure and temperature. As the outlet pressure is in the range of a few Pascals, the pressure effect has been neglected; thus, influencing parameter is the actual turbine exit temperature.

As compressor work is a function of the mechanical efficiency of the turbocharger and turbine work, the turbine work was estimated. Literature suggests that the mechanical efficiency of most of the turbochargers is 92 per cent [**23**].

The turbine work is dependent on exhaust flow, specific heat at constant pressure and the turbine inlet and outlet temperature difference. Mass flows across the compressor and turbine remain the same for a particular load. From exhaust composition, specific heat values were calculated. Table 7 presents the results on the turbine efficiency.

On Engine 2, the turbine efficiency, as calculated analytically, was found to be 71 per cent at 110 kW, which is not consistent with the compressor efficiency at this load, which was around 76 per cent. This difference may probably be attributed to the assumptions made (compressor efficiency from literature set at 92 per cent) in estimating the correct turbine outlet temperature. Assuming the compressor efficiency as 86 per cent, the calculated turbine efficiency matches with the expected results.

While the above approach is an indirect method to estimate the turbine efficiency which depends on the assumptions made, a rather direct measurement of the turbine exit temperature would be appropriate. It must be mentioned that the heat loss pattern during the expansion process will not remain the same for all sets of loads; even small errors in temperature of even a few percent would give considerable variation in turbine efficiency calculation.

The turbine efficiency is calculated using equation (2) which depends on the turbine inlet, exit, and the isentropic temperatures. Presently, the inlet temperature is accurate while the exit temperature is in error. The difference between the inlet and exit is about 200 K at the rated condition. Based on the compressor work, the compressor exit temperature should have been in the range of 561 K amounting to a temperature difference of 43 K. Therefore, in this study, the compressor performance has been evaluated, while similar performance evaluation of the turbine is not possible as the true temperature drop across turbine could not be measured due to turbine casing cooling as designed by the engine manufacturer. Even though the exact performance of the turbine is not evaluated, this study has provided an accurate estimation of compressor performance and indirectly estimates the turbine performance. Further study is required

Table 7 Estimated turbine efficiency for Engine 2

	Measured parameters on turbine				Estimated based on turbine work		
Load (kW)	T_3 (K)	T_4 (K)	P_4/P_3	Isentropic temperature, T_{4s} (K)	Turbine work	Corrected temperature, T_4 (K)	Calculated efficiency, η_T (%)
0	743	585	0.97	738	0.31	740	0.64
20	819	642	0.92	802	1.06	810	0.53
30	823	645	0.88	798	2.63	804	0.76
45	825	651	0.83	788	4.66	796	0.77
50	815	645	0.82	776	4.98	784	0.79
60	826	657	0.80	784	5.89	792	0.79
70	832	650	0.80	787	6.58	795	0.82
80	834	651	0.77	784	8.89	788	0.92
90	858	663	0.76	804	9.20	812	0.85
100	876	672	0.75	817	9.48	831	0.78
110	881	679	0.74	818	9.72	837	0.71

in order to generate the turbine performance maps due to the above limitation.

5.3 Operating characteristics of the turbocharger with producer gas engine

Figure 10 shows the comparison of the operating characteristics of the turbocharger with NG and producer gas as fuels. The compressor map for Holset 4 LGK/557 turbocharger with NG on GTA-855-G (i.e. Engine 2) [**24**, **25**] is used as a reference. The turbo flow is corrected for pressure at 101.3 kPa and temperature for 288 K. Increasing the speed of the turbocharger can influence the efficiency and the pressure ratio. It is important to state that the speed of the turbine is an important parameter which needs to be monitored. This issue may have a significant bearing on the de-rating observed in producer gas operation, thus ensuring increase in the power output for the given cylinder volume.

Figure 11 compares the SEC with NG and producer gas as fuels. It is evident from Tables 3 and 4 along with Fig. 11 that the SEC is lower by about 15 per cent in NG mode and also the power output is higher. These are related to the properties of the fuel that influence the combustion process inside the engine cylinder. The adiabatic flame temperature and product-to-mole fraction ratio have an influence on the cylinder pressure, which has an influence on the power output [**11**].

Figure 12 presents the results on the emissions from the engine exhaust. The data presented are normalized at 5 per cent oxygen level in the dry exhaust. These measurements are without any catalytic converter on the exhaust. The CO levels vary over the load range from 20 g/kWh to about 90 g/kWh. It is interesting to note that around 110 kW, which is nearly the peak load condition, the CO level has increased. This sudden increase is related to A/F approaching the nearly the stoichiometric condition leading to incomplete combustion. The NOx levels are under 2.5 g/kWh [**20**]. Further studies are necessary on the emission values to understand this behaviour.

This study has provided an insight towards understanding the performance of turbocharged gas engines with producer gas as the fuel. It is evident that there is significant scope for further work in the area of related to the increase of the pressure ratio of the gas–air mixture to enhance the output. Further investigations are necessary towards measuring the turbine speed and other related parameters towards enhancing the turbocharger performance by choosing the right operating conditions with respect of both speed and efficiency. In the anticipated future, studies coupling with in-cylinder pressure measurements would ensure addressing critical operating parameters with respect to rate of pressure rise, knocking, if any, emissions, and aspects of efficiency.

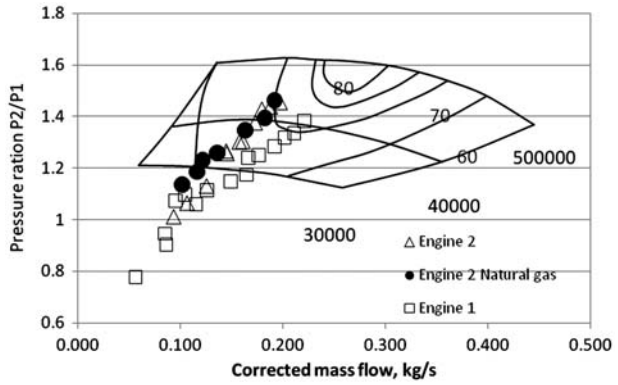

Fig. 10 Comparison of operating characteristics using NG and producer gases as the fuels

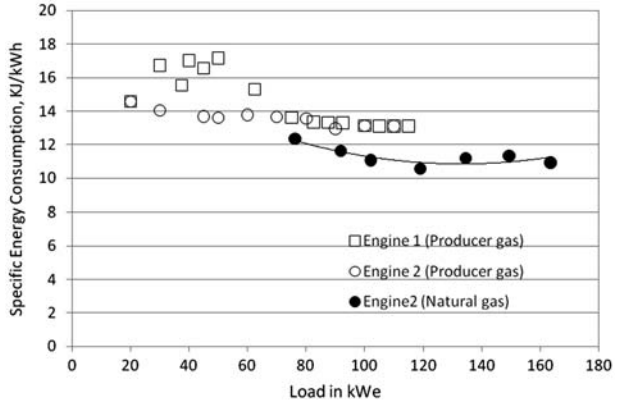

Fig. 11 Comparison of SEC with NG

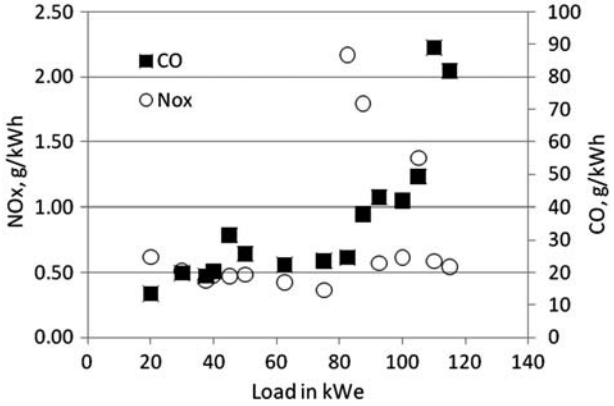

Fig. 12 Emission from the engine exhaust (Engine 1)

6 CONCLUSIONS

The performance of a turbocharger using producer gas has been tested and thermodynamic analysis carried out. The compressor performance has been mapped and compared with that available for NG operation. It has been found that the compressor efficiency is about 70 per cent and the pressure ratio achieved about 1.45. Compared with the naturally aspirated condition, the turbocharged operation performed with 35 per cent enhanced power output. Aspects related to turbine efficiency are highlighted and need further work.

REFERENCES

1 **MNRE.** 2010, available from http://mnre.nic.in [viewed December 2010].
2 **Dasappa, S., Paul, P. J., Mukunda, H. S., Rajan, N. K. S., Sridhar, G.,** and **Sridhar, H. V.** Biomass gasification technology – a route to meet energy needs. *Curr. Sci.*, 2004, **87**(7), 908–916.
3 **Knoef, H. A. M.** (Ed.) *Handbook of biomass gasification*, 2005 (Biomass Technology Group, Netherlands).
4 **Sridhar, G., Dasappa, S., Sridhar, H. V., Paul, P. J., Rajan, N. K. S., Prakasam Kummar, V. S.,** and **Chandra Mohan, V.** Green electricity - a case study of a grid linked independent power producer. In Proceedings of the 15th European Biomass Conference & Exhibition, Berlin, Germany, 7–11 May 2007, pp. 2256–2261.
5 **Dasappa, S., Sridhar, G., Sridhar, H. V., Rajan, N. K. S., Paul, P. J.,** and **Arvind, U.** Producer gas engines proponent of clean energy technology. In Proceedings of the 15th European Biomass Conference & Exhibition, Berlin, Germany, 7–11 May 2007, pp. 976–981.
6 **Baliga, B. N., Dasappa, S., Mukunda, H. S.,** and **Shrinivasa, U.** Gasifier based power generation: technology and economics. *Sadhana Acad. Proc. Engng Sci.*, 1993, **18**(1), 57–75.
7 **Ravindranath, N. H., Somashekar, H. I., Dasappa, S.,** and **Jaysheela Reddy, C. N.** Sustainable biomass power for rural India: case study of biomass gasifier for village electrification. *Curr. Sci.*, 2004, **87**(7), 932–941.
8 **Ghosh, S., Das, T. K.,** and **Jash, T.** Sustainability of decentralized woodfuel-based power plant: an experience in India. *Energy*, 2004, **29**(1), 155–166.
9 **Shashikanta** and **Parikh, P. P.** Spark ignited producer gas and dedicated CNG engine-technology development and experimental performance. SAE paper 1999-01–3515 (SP-1482), 1999.
10 **Heywood, J. B.** *Internal combustion engine fundamentals*, International edition, 1988 (McGraw-Hill, New York).
11 **Dasappa, S.** On the estimation of power from a diesel engine converted for gas operation a simple analysis. In Proceedings of the 17th National Conference on IC Engines and Combustion, Suratkal, India, 18–20 December 2001, pp. 167–174.
12 **Tinaut, F. V., Melgar, A., Horrillo, A.,** and **Rosa, A. D.** de la. Method for predicting the performance of an internal combustion engine fuelled by producer gas and other low heating value gases. *Fuel Process. Technol.*, 2006, **87**(2), 135–142.
13 **Ahrenfeldt, J., Foged, E. V., Strand, R.,** and **Henriksen, U. B.** Development and test of a new concept for biomass producer gas engines. Risø-R-1728 (EN) Risø National Laboratory for Sustainable Energy, Technical University of Denmark, February 2010.
14 **Sridhar, G.** *Experimental and modeling studies of producer gas based spark-ignited reciprocating engines.* PhD Thesis, Indian Institute of Science, Bangalore, 2003.
15 **Sridhar, G., Sridhar, H. V., Dasappa, S., Paul, P. J., Rajan, N. K. S.,** and **Mukunda, H. S.** Development of producer gas engines. *Proc. IMechE, Part D: J. Automobile Engineering*, 2005, **219**(3), 423–438.
16 **Lettner, F., Timmerer, H.,** and **Haselbacher, P.** Biomass gasification – state of the art description, Guideline for safe and eco-friendly biomass gasification Intelligent Energy – Europe (IEE), 2007, Report, EIE/06/078/SI2.447511.
17 **Malik, A., Singh, L.,** and **Singh, I.** Utilisation of biomass as engine fuel. *J. Sci. Ind. Res.*, 2009, **68**(10), 887–890.
18 **Ramadhas, A. S., Jayaraj, S.,** and **Muraleedharan, C.** Power generation using coir-pith and wood derived producer gas in diesel engines. *Fuel Process. Technol.*, 2006, **87**(10), 849–853.
19 **Bhattacharya, S. C., San, S. H.,** and **Pham, H. L.** A study on a multi-stage hybrid gasifier-engine system. *Biomass Bioenergy*, 2001, **21**(6), 445–460.
20 Cummins Gas Engines Service Manual, Cummins India Ltd., Pune, India, 2003.
21 http://cumminsindia.com:8080/xsql/cumminsIndia/CIL/PGBU/gas_engines.html (viewed December 2010).
22 **ABETS.** *Biomass to energy – the science and technology aspects of IISc bio-energy systems*, 2003 (ABETS, Indian Institute of Science, Bangalore).
23 **Maclnnes, H.** *Turbochargers*, H.P. Books, 1978 (The Berkley Publishing Group, New York, USA).
24 Holset Engineering Co. Ltd., Compressor performance (shared by Cummins India Ltd.).
25 **Mazumdar, I.** *Performance evaluation of a turbocharger for producer gas operation.* MTech Thesis, Tezpur University, 2005.

APPENDIX

Notations

C_p	specific heat
$\dot{m}_a$	mass flowrate of air
$\dot{m}_e$	total mass flow exiting from the engine exhaust.
$\dot{m}_g$	mass flowrate of gas

P_1 to P_5	pressure at various locations on the turbocharger
T_s	isentropic temperature
T_1 to T_5	temperature at various locations on the turbocharger
W_c	compressor work
W_T	turbine work
η_c	compressor efficiency
η_t	turbine efficiency
η_m	turbine efficiency